

DETC2009-87457

## SIMULTANEOUS TRAJECTORY TRACKING AND STIFFNESS CONTROL OF CABLE ACTUATED PARALLEL MANIPULATOR

Kun Yu, Leng-Feng Lee and Venkat N. Krovi\*  
Department of Mechanical & Aerospace Engineering  
State University of New York at Buffalo  
Buffalo, New York, USA

### ABSTRACT

Cable-actuated parallel manipulators combine benefits of large workspaces, significant payload capacities and high stiffness by virtue of the cable actuation. However, redundant/surplus cables are required to overcome the unidirectional nature of forces exertable by cables. This leads to actuation redundancy which needs to be resolved in order to realize some of the benefits.

We study the implication of using actuation redundancy to tailor the workspace (task space) stiffness of the cable robot system. Suitable trajectory tracking control schemes are developed that additionally achieve secondary goal of active stiffness control to improve disturbance rejection, under positive control input constraint. We demonstrate the performance of these control schemes using a point-mass cable robot system modeled within a virtual prototyping (VP) implementation framework.

### 1 INTRODUCTION

Cable-robot manipulators are formed by replacing the multiple sets of articulated-legs of a parallel-architecture manipulator with cables. This allows the end-effector/platform motion trajectories and exerted forces to be controlled by extending or retracting the various cables. However, cable robot systems can function only when the cables are in tension. Additional active cables are typically introduced, leading to surplus of actuators over degrees of freedom [1].

On one hand, this creates indeterminacy in terms of the force-distribution required to achieve desired end-effector motion. On the other hand, without careful coordination, substantial internal forces can build up within the close-kinematic-loops. Effective resolution of this redundancy, by way of satisfying auxiliary constraints or secondary optimization criteria, becomes necessary for control. Suitable developments of actuation redundancy resolution schemes offer not only the capability of performing the primary task

but also to redistribute cable-actuation forces to satisfy secondary criteria. Hence such methods have found application for eliminating singularities within workspace [2], reducing the chance of system failure, and realizing optimal actuation distribution and power consumption among the actuators [3], or for enable active stiffness control in terms of modulating internal actuation distribution [1, 4].

While redundantly-actuated parallel robots have been treated in the literature previously, the unilateral nature of the cable-tension constraint creates challenges. Many parallels exist between the unilateral tension requirements and unidirectional normal-force constraints arising in multifingered hands and multilegged walkers [5]. Several solution approaches have been proposed to perform redundancy resolution while maintaining positive tensions, including feedback linearization approaches [6] and time-optimal trajectory control [7].

At the same-time, several authors have studied the end-effector stiffness of cable robots. As in other robotic manipulators, stiffness is a very important measure of the manipulator's structural rigidity and trajectory-following performance (and more-importantly disturbance-rejection). Albus et al. performed the first study of stiffness for cable robots in [8] and later used the result for the design and development of the NIST RoboCrane. More recently, Verhoeven *et al.* [9] presented a paper on the stiffness of cable actuated robots. Stiffness control strategies seek to provide relationships between position error and external force exerted by the end-effector. Stiffness control strategy can be thought as a special case of impedance control that considers only the steady state force/displacement relationship. However, it does not adequately describe nor control the transient response resulting from the dynamic behavior of the system [10]. Active stiffness control strategies have been developed to achieve desired end-effector stiffness using redundant actuation [4] for general robotic manipulators.

\* Corresponding author, Phone: (716) 645-1430, Fax: (716) 645-3668, Email: vkrovi@eng.buffalo.edu.

However, to the best of our knowledge, no one has explicitly considered the use of active stiffness control using the redundant actuation to achieve desired end-effector stiffness in cable robots. Such control now offers the possibility for the robot to dynamically counteract uncertain and unmodeled disturbances. Further, since stiffness-control using redundant actuation is formulated in the null-space of the system dynamics, linear superposition over the trajectory tracking control guarantees natural prioritization of the trajectory following task. We will explore some of these aspects further in this paper.

The rest of paper is organized as follows. The system description and modeling efforts are presented in Section 2. Section 3 explains the identification method for the interaction force. The simulation framework is explained in Section 4, with numerical simulations presented in Section 5, followed by concluding remarks in Section 6.

## 2 CABLE ROBOT SYSTEM

### 2.1 Kinematic and Dynamic Equations of Motion

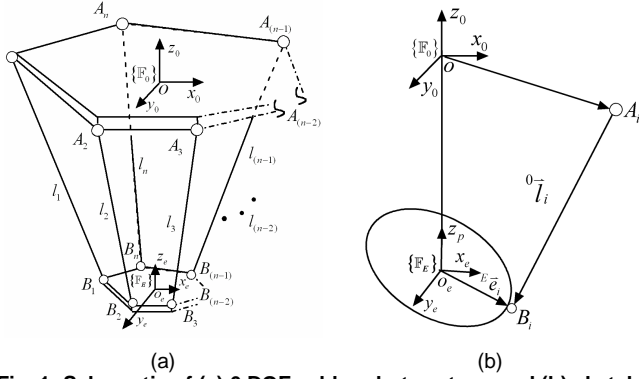


Fig. 1: Schematic of (a) 6 DOF cable robot system; and (b) sketch of cable  $i$  and its related position vectors.

Figure 1(a) shows a spatial 6-dof cable robot actuated by  $n$  identical cables. Following [11], the lower plate, considered to be the moving end-effector, is connected by  $n$  identical cables to the upper fixed base at connection-points  $A_i$  and  $B_i$ ,  $i = 1, 2, \dots, n$ , distributed at the vertices of an arbitrary polygon. Several closed kinematic loops are formed by the cables. Two Cartesian coordinate system:  $\mathbb{F}_0(O, x_0, y_0, z_0)$  attached to the base with the origin located at the center, and  $\mathbb{F}_E(O_e, x_e, y_e, z_e)$  attached to the moving platform (end-effector). The location of the  $i^{\text{th}}$  external and onboard cable connection be denoted by  ${}^0B_i$  and  ${}^0A_i$ . The Jacobian of cable robot may be derived as:

$$\dot{l} = J \dot{X} \quad (1)$$

where

$$J = \begin{bmatrix} \hat{l}_1^T & ({}^0e_1 \times \hat{l}_1)^T \\ \hat{l}_2^T & ({}^0e_2 \times \hat{l}_2)^T \\ \hat{l}_3^T & ({}^0e_3 \times \hat{l}_3)^T \\ \vdots & \vdots \\ \hat{l}_n^T & ({}^0e_n \times \hat{l}_n)^T \end{bmatrix} = \begin{bmatrix} \hat{l}_1^T & -(\hat{l}_1 \times {}^0R_E {}^Ee_1)^T \\ \hat{l}_2^T & -(\hat{l}_2 \times {}^0R_E {}^Ee_2)^T \\ \hat{l}_3^T & -(\hat{l}_3 \times {}^0R_E {}^Ee_3)^T \\ \vdots & \vdots \\ \hat{l}_n^T & -(\hat{l}_n \times {}^0R_E {}^Ee_n)^T \end{bmatrix} \quad (2)$$

and

$$\dot{X} = [\dot{x} \quad \dot{y} \quad \dot{z} \quad \dot{\omega}_x \quad \dot{\omega}_y \quad \dot{\omega}_z]^T, \quad \dot{l} = [\dot{l}_1 \quad \dot{l}_2 \quad \dot{l}_3 \quad \dots \quad \dot{l}_n]^T \quad (3)$$

where  ${}^0\bar{l}_i$  is the position vector of  $i$ th cable ( $i=1,2,\dots,n$ ) with respect to frame  $\{\mathbb{F}_0\}$ ,  $\hat{l}_i = {}^0\bar{l}_i / \|{}^0\bar{l}_i\|$  is the unit length vector of  $i$ th cable.  ${}^Ee_i$  is the position of the  $i$ -th onboard cable connector relative to the end-effector coordinate frame  $\{\mathbb{F}_E\}$ .  $\dot{l}_i$  represents the velocity of  $i$ th cable, and  $\dot{X} = [\dot{x} \quad \dot{y} \quad \dot{z} \quad \dot{\omega}_x \quad \dot{\omega}_y \quad \dot{\omega}_z]^T$  is the velocity vector for the reference point in moving platform with respect to base frame  $\{\mathbb{F}_0\}$ . A simplified representation of  $\dot{l} = J \dot{X}$  can be obtained for cable robots with point mass moving platform, as:

$$J = \begin{bmatrix} \hat{l}_1^T & \hat{l}_2^T & \hat{l}_3^T & \dots & \hat{l}_n^T \end{bmatrix}^T \quad (4)$$

$$\dot{X} = [\dot{x} \quad \dot{y} \quad \dot{z}]^T, \quad \dot{l} = [\dot{l}_1 \quad \dot{l}_2 \quad \dot{l}_3 \quad \dots \quad \dot{l}_n]^T \quad (5)$$

Furthermore, when dealing with the planar case,  $l_i$ ,  ${}^0p_i$ ,  ${}^0b_i$ ,  ${}^0X_E$  and  ${}^Ee_i$ ,  ${}^0X_E = [x \quad y \quad \theta]^T$  are vectors in the plane and the orientation is given by

$${}^0R_E = R(\theta) = \begin{bmatrix} c\theta & -s\theta & 0 \\ s\theta & c\theta & 0 \\ 0 & 0 & 1 \end{bmatrix} \quad (6)$$

Further following [11], we can also obtain the dynamic equations of motion (EOM) of cable robot system as:

$$M(X)\ddot{X} + h(X, \dot{X}) + g(X) = -J^T F \quad (F \geq 0) \quad (7)$$

where  $M(X)$  is the inertial matrix,  $h(X, \dot{X})$  term represents the Coriolis and centrifugal forces,  $g(X)$  represents the external forces, including gravitational force, and  $F$  is the cable tension force.

### 2.2 Feedback Linearization

As an example of a simple mechanical system [12], the feedback linearization control law can be derived for such systems in a straightforward manner. We consider a PD controller based feedback linearization technique to meet the trajectory tracking requirement. Let  $X_d(t)$ ,  $\dot{X}_d(t)$  and  $\ddot{X}_d(t)$  represents the desired trajectory information and error between actual and desired trajectory be defined as:

$$e = X_d(t) - X(t) \quad (8)$$

Substituting  $\ddot{X} = \ddot{X}_d + K_p e + K_d \dot{e}$  into the EOM we can solve for the control input as:

$$F_p = (-J^T)^\# [M(X)(\ddot{X}_d + K_p e + K_d \dot{e}) + h(X, \dot{X}) + g(X)] \quad (9)$$

which yields task-space error dynamics which can be designed by pole-placement as:

$$M(X)(\ddot{e} + K_p \dot{e} + K_d \dot{e}) = 0 \quad (10)$$

### 2.3 Redundancy Resolution

Effective actuation-redundancy resolution schemes can be developed for cable robot, formulated based on pseudo-inverse solution to the system equations of motion. Let  $W = [f \ m]^T$  represent the vector of output wrenches (forces and moments) on the end-effector,  $F = [F_1 \ F_2 \ \dots \ F_n]^T$  represents the vector of tensions applied by cables, according to principle of virtual work:

$$W_{(m \times 1)} = -J_{(m \times n)}^T F_{(n \times 1)} = S_{(m \times n)} F_{(n \times 1)}, \quad (F \geq 0) \quad (11)$$

A general pseudo-inverse solution for Eq. (11) can be written as

$$F = S^\# W + (I - S^\# S)z = F_p + F_h \quad (12)$$

where  $I$  is  $n \times n$  identity matrix,  $z$  is an arbitrary  $n$ -vector, and  $S^\#$  is Moore-Penrose pseudoinverse of  $S$ . Since the cable robot system under our consideration is almost always redundantly actuated (underconstrained), which means  $m < n$ ,  $S^\#$  can be computed as  $S^\# = S^T (SS^T)^{-1}$ . The first term of Eq. (12),  $F_p$  corresponds to the particular solution. The second term,  $F_h$ , corresponds to the homogeneous solution that maps  $z$  to the null space of  $S$ . When the second term  $F_h = 0$ , we have  $F = F_p$ , which corresponds to least squares minimum-norm solution to the system of equations. However, the positiveness of this solution is undetermined, which implies that unidirectional force constraint may be violated. Since  $F_h$  can take on any value, there will result in infinite set of possible solutions to the system. As shown in [13, 14],  $F_p$  can be interpreted as the min-norm equilibrating force field while  $F_h$  as internal force which does not contribute to the effective work to the environment. Most importantly, the positiveness of forces can be ensured by properly modulating internal actuation distribution, which can be non-unique.

#### 2.3.1 Minimal Parameterization of Null Space

In Eq.(12), let  $H = (I - S^\# S)$ , Typically  $H$  matrix is found to be rank deficient:  $\text{rank}(I - S^\# S) = (n - m) < n$ , which means non-independent components exist within the null space of  $S$ . As the result of that, discontinuity may result in  $z$  [15] due to different set of  $(n - m)$  independent columns of  $H$  chosen for  $S$  in each iterative steps. Thus, in this section, we present an approach to find the minimal parameters to uniquely represent the null space solution. To solve this problem, we can perform singular value decomposition (MATLAB routine SVD) to obtain the full rank nullspace component of the system:

$$H = U \Delta V^T \quad (13)$$

where  $U$  and  $V$  are  $n \times n$  orthogonal matrices, and  $\Delta$  is the diagonal matrix contains the singular value of  $H$  in the form  $\Delta = \text{diag}\{\sigma_1, \sigma_2, \dots, \sigma_{(n-m)}, 0, \dots, 0\}$  with  $\sigma_i > 0, i = 1, 2, \dots, n - m$ .

We choose  $N(S) = [U_1 \ U_2 \ \dots \ U_{(n-m)}]$  as the first  $(n - m)$  columns of  $U$  matrix corresponding to first  $(n - m)$  non-zero singular values. Obviously  $\text{rank}(N(S)) = n - m$  since  $U$  is orthogonal matrix), then, an equivalent expression for Eq. (12) becomes

$$F = S^\# W + \sum_{j=1}^{n-m} \alpha_j N_j = F_p + N(S)\bar{\alpha} \quad (14)$$

where  $N(S) = [n_1 \ n_2 \ \dots \ n_i]_{n \times (n-m)}$  denotes the full rank null space or kernel matrix of  $S$ , and  $\bar{\alpha} = [\alpha_1 \ \alpha_2 \ \dots \ \alpha_i]^T$  is an arbitrary  $(n - m)$  vector. Here,  $i = (n - m)$  where  $n$  is the number of cables and  $m$  is the dimension of the Cartesian space or rank of matrix  $S$ .

#### 2.3.2 Tension Optimization Formulation

In cases, least squares minimum-norm solution  $F_p$  results in some negative tensions, certain criteria is needed to choose a proper homogeneous solution  $F_h$  to guarantee the positiveness of  $F$ . Specifically, we can optimize the tension among cables by imposing proper objective function and considering components of  $\bar{\alpha}$  vector in Eq. (14) as design variables in the optimization processes. The optimization schemes can be formulated as a linear program as follows.

$$\begin{aligned} \text{Min}_{\bar{\alpha}}: & \quad W_f^T F \\ \text{where: } & \quad F = S^\# W + \sum_{j=1}^{n-m} \alpha_j N_j = F_p + N(S)\bar{\alpha} \\ \text{subject to: } & \quad -N(S)\bar{\alpha} \leq F_p \end{aligned} \quad (15)$$

$W_f$  is a weighting matrix. For example, If all components of  $W_f$  are 1, the objective function becomes  $(F_1 + F_1 + \dots + F_n)$ . Alternatively, Eq. (15) can be reformulated as follows

$$\begin{aligned} \text{Min}_{\bar{\alpha}}: & \quad W_f^T \bar{\alpha} \\ \text{subject to: } & \quad -N(S)\bar{\alpha} \leq F_p \end{aligned} \quad (16)$$

## 3 ACTIVE STIFFNESS CONTROL

### 3.1 Cartesian Stiffness of Cable Robot System

The forces and moments acting on the end-effector, or the reaction forces and moments exerted to the environment by the end-effector,  $W = [f \ m]^T$  and deflection of the end-effector  $\delta X$  caused by  $W$  can be related by a stiffness matrix  $K_x$  as:

$$dW = K_x dX \quad (17)$$

where  $K_x$  is called Cartesian or task space stiffness matrix. Similarly, tension forces exerted by cables  $F = [F_1 \ F_2 \ \dots \ F_n]^T$  and displacement within cables  $\delta l = [\delta l_1 \ \delta l_2 \ \dots \ \delta l_n]$  caused by  $F$  can be related by a stiffness matrix (cables are assumed to have linear stiffness property)  $K_i$  as

$$dF = K_l dl \quad (18)$$

where  $K_l$  is called joint space stiffness matrix, and it is usually a diagonal matrix composed of cable stiffness constants.

Now we can get relationship between joint torques and the end-effector force according to cable system dynamic equation

$$W = SF \quad (19)$$

By taking differentiation of Eq. (19), we get

$$dW = (dS)F + S(dF) \quad (20)$$

and substitute Eq. (17) and Eq. (18) into Eq. (20), we have

$$K_x dX = (dS)F + SK_l(dl) \quad (21)$$

where,  $dS = \sum_{i=1}^6 \frac{\partial S}{\partial x_i} dx_i$ , which is derived by taking

differentiation upon task space variables  $X = (x_1, x_2, \dots, x_6)$ .

Then, along with the Jacobian  $J = dl/dX$ , Eq. (21) can be rewritten as

$$K_x = K_g + K_c \quad (22)$$

where

$$K_g = \left[ \frac{\partial S}{\partial x_1} F \quad \frac{\partial S}{\partial x_2} F \quad \dots \quad \frac{\partial S}{\partial x_6} F \right] \quad (23)$$

$$K_c = SK_l J = -J^T K_l J \quad (24)$$

Eq. (22) represents the relationship of mapping between Cartesian stiffness and joint stiffness. The term  $K_g$  includes the differential Jacobian (a Hessian-3D tensor) and internal actuation force. Since it is depends on configuration and cable forces, it can be nonpositive definite and asymmetric.

From the relationship of mapping between Cartesian stiffness and joint stiffness derived above, we can see that Cartesian stiffness is not only related to changes in joint stiffness, but also to changes in system configuration as well as changes in actuation forces or torques in joints. Kao *et al.* [16] termed this mapping between Cartesian stiffness and joint stiffness as conservative congruence transformation (CCT), and they pointed out the incompleteness of the conventional formulation proposed by Salisbury in [17] based on the fact that work done in joint space and Cartesian space within a robotic system should obey the law of conservation of energy. In the conventional mapping between Cartesian stiffness and joint stiffness, the importance of changes in actuation forces or torques to the total stiffness matrix is omitted; however, its contribution to the total stiffness of a system can be very significant, especially in the case of baised-payload bearing and a actuation-redundant system.

### 3.2 Active Stiffness Control Schemes

Effective stiffness schemes can be formulated as optimization problem by taking advantage of the indeterminacy of actuation forces resulting from actuation redundancy. We can achieve different goals by formulating different objective functions in optimization.  $\bar{\alpha}$  vector in Eq. (14) is design variable in optimization process, following shows general form of four schemes based on different scenario. Before we formulate the optimization schemes, first we need to rewrite Eq. (22) into the following form:

$$\overline{K_x} = \overline{K_g} + \overline{K_c} \quad (25)$$

where

$$\overline{K_x} = [K_x(:,1) : K_x(:,2) : \dots : K_x(:,m)]^T_{(m \times (m \times 1))} \quad (26)$$

$$\overline{K_c} = [K_c(:,1) : K_c(:,2) : \dots : K_c(:,m)]^T_{(m \times (m \times 1))} \quad (27)$$

$$\overline{K_g} = HF = H(F_p + N(S)\bar{\alpha}) = HF_p + HN(S)\bar{\alpha} \quad (28)$$

$$H = \left[ \frac{\partial S}{\partial x_1} : \frac{\partial S}{\partial x_2} : \dots : \frac{\partial S}{\partial x_m} \right]^T_{m \times (m \times n)}$$

Substituting Eq. (28) into Eq. (25), yields  $\overline{K_x}$  with implicit  $\bar{\alpha}$ :

$$\overline{K_x} = \overline{K_c} + HF_p + HN(S)\bar{\alpha} \quad (29)$$

Now, we can define the general form of the optimization using Eq. (29) shown in the next section.

#### 3.2.1 Minimal Force Distribution with Desired Stiffness

$$\text{Min}_{\bar{\alpha}} : W_f^T \bar{\alpha}$$

$$\text{Where : } \overline{K_x} + HF_p + HN(S)\bar{\alpha} = c \quad (30)$$

$$\text{Subject to : } -N(S)\bar{\alpha} \leq F_p$$

$c$  is constant that represents desired end-effector stiffness.  $W_f$  is a weighting matrix. However, this scheme is greatly limited when the number of extra cables is less than  $(\gamma-1)$ ,  $\gamma$  is the number of independent components of desired stiffness matrix. As we can prove the number of extra cables denotes the dimension of design variable  $\bar{\alpha}$ , However, in most cases, too many extra cables is not desired, as it will impose higher possibility of cable interference and greatly limit the workspace. As the result of that, a feasible solution does not always exist in Eq. (30), which means desired stiffness can not be achieved in most designs under this strict criteria. Due to its ineffectiveness and limitation, we will not consider this approach as candidate for active stiffness control schemes.

### 3.3 Weighted Stiffness Matrix Approach

The error between the desired stiffness and actual stiffness can be defined as:

$$dK_x = \overline{K_x} - \overline{K_{xd}} \quad (31)$$

Our objective is to reduce  $dK_x$  by controlling the redundantly actuated forces exerted by cables. However, as mentioned earlier, it is not always possible to realize the desired stiffness in all directions of Cartesian space. Thus, it is necessary that an order of priority can be specified among stiffness of different directions. In this way, flexibility and usability of the control scheme are greatly enhanced. For this purpose, we can formulate the optimization problem as a Quadratic programming problem as follows:

$$\text{Min}_{\bar{\alpha}} \quad \frac{1}{2} dK_x^T W_k dK_x$$

$$\text{where } \overline{K_x} = \overline{K_c} + HF_p + HN(S)\bar{\alpha} \quad (32)$$

$$\text{s.t. } -N(S)\bar{\alpha} \leq F_p$$

$$W_k = \begin{bmatrix} w_{11} & 0 & \dots & 0 \\ 0 & w_{22} & \dots & 0 \\ \vdots & \vdots & \ddots & \vdots \\ 0 & 0 & 0 & w_{nn} \end{bmatrix}_{\left(\frac{n(n+1)}{2}, \frac{n(n+1)}{2}\right)} \quad \text{with } \sum_{i=1}^{\frac{n(n+1)}{2}} w_{nn}^2 = 1 \quad (33)$$

where  $dK_x$  is a  $(n(n+1)/2 \times 1)$  vector formed by the unique elements of the stiffness matrix, since the stiffness matrix is symmetric, for a stiffness with  $n$  dimension the number of unique elements is  $n(n+1)/2$ ,  $W_k$  is a diagonal weighting matrix with its elements corresponding to each unique elements in  $dK_x$ .

## 4 SIMULATION FRAMEWORK

### 4.1 Virtual Simulation and Analysis Framework

Virtual Prototyping has rapidly gained popularity and become a crucial part of most engineering design processes [18]. In this section, we will discuss the development of an integrated analysis framework (using MATLAB/ Simulink/ MSC. visualNastran) for virtual simulation of our design and testing of redundancy resolution and stiffness control schemes (See Fig. 2). In the future this implementation is also intended to form the basis for the real-time, hardware-in-the-loop simulation of a mechanical model of the system.

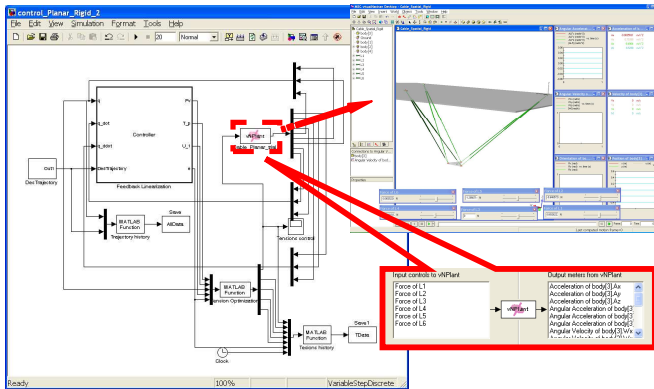


Fig. 2: MATLAB/Simulink, MSC. visualNastran integrated analysis framework.

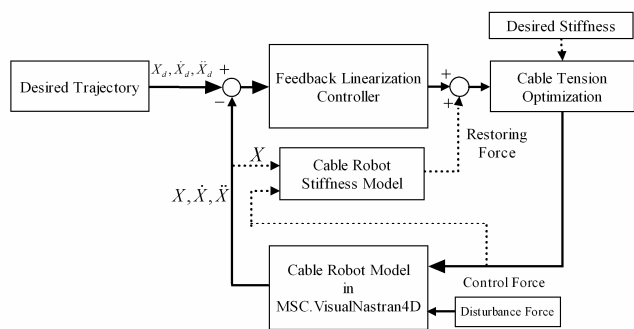


Fig. 3: SIMULINK block diagram of overall simulation routine.

A block diagram of our simulation routine is shown in Fig. 3. It is composed of seven blocks: desired trajectory, feedback linearization controller, cable tension optimization, cable robot model in MSC. visualNastran 4D, Desired stiffness, cable robot stiffness model and disturbance force. The *Cable Robot model in MSC. visualNastran 4D* block contains the virtual prototype of cable robot system built in MSC. visualNastran 4D, it serves as the plant being controlled by cable forces input that are generated in MATLAB/Simulink in the simulation routine. This block outputs simultaneous

information of the robot system in position, velocity and acceleration levels, which serves as the feedback input to the *Feedback Linearization Controller* block, such that correcting control inputs to the cable robot will be generated according to desired trajectory information specified in *desired trajectory* block. The *Cable Tension Optimization* block serves as the decision making and secondary tasks block to regulate control inputs from *Feedback Linearization Controller* block depending on different redundancy resolution schemes implemented. In our work, it is used to achieve minimal forces exertion among cables and active stiffness control in the premise of maintaining cables in tension. The *Desired Stiffness* block is used to specify desired end-effector stiffness of cable robot in active stiffness control. The *Cable Robot Stiffness* block contains the stiffness model of cable robot developed in and serves a part of active stiffness control scheme. Inputs of this block include the position information, input control cable forces, cables stiffness constant and configuration information of current system. The output of this block is the resorting force corresponding to controlled stiffness along with position error generated by disturbance force from *Disturbance Force* block. This resorting force serves as the compensation in disturbance rejection scenario.

## 5 CASE STUDIES

### 5.1 Planar point-mass cable robot

Several case studies are currently in progress (for planar point-mass, planar rigid-body, spatial point-mass and spatial-rigid-body). We will however report the results in the context of a planar point mass cable robot system as shown in Fig. 4, the end-effector is modeled as a point mass and attached by three cables, which are actuated by one motor separately in a plane. The three motors forming the base are located at (0, 0) m, (0.6, 0) m, and (0.3, 0.52) m. The initial position of the end-effector is located at (0.35, 0.173) m, which is the center of the equilateral triangle formed by the boundary of the base. As we can see, this system is fully constrained. It has one redundant actuation since the end-effector has two DOF while it is driving by three cables.

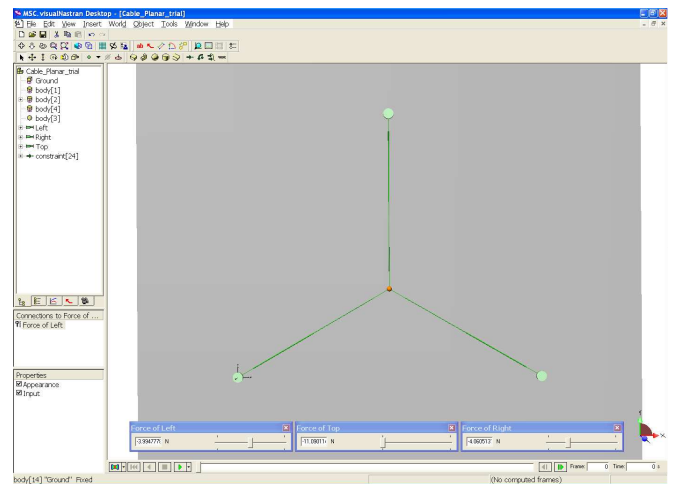


Fig. 4: Virtual Model of a planar point-mass cable robot system model in visualNastran.

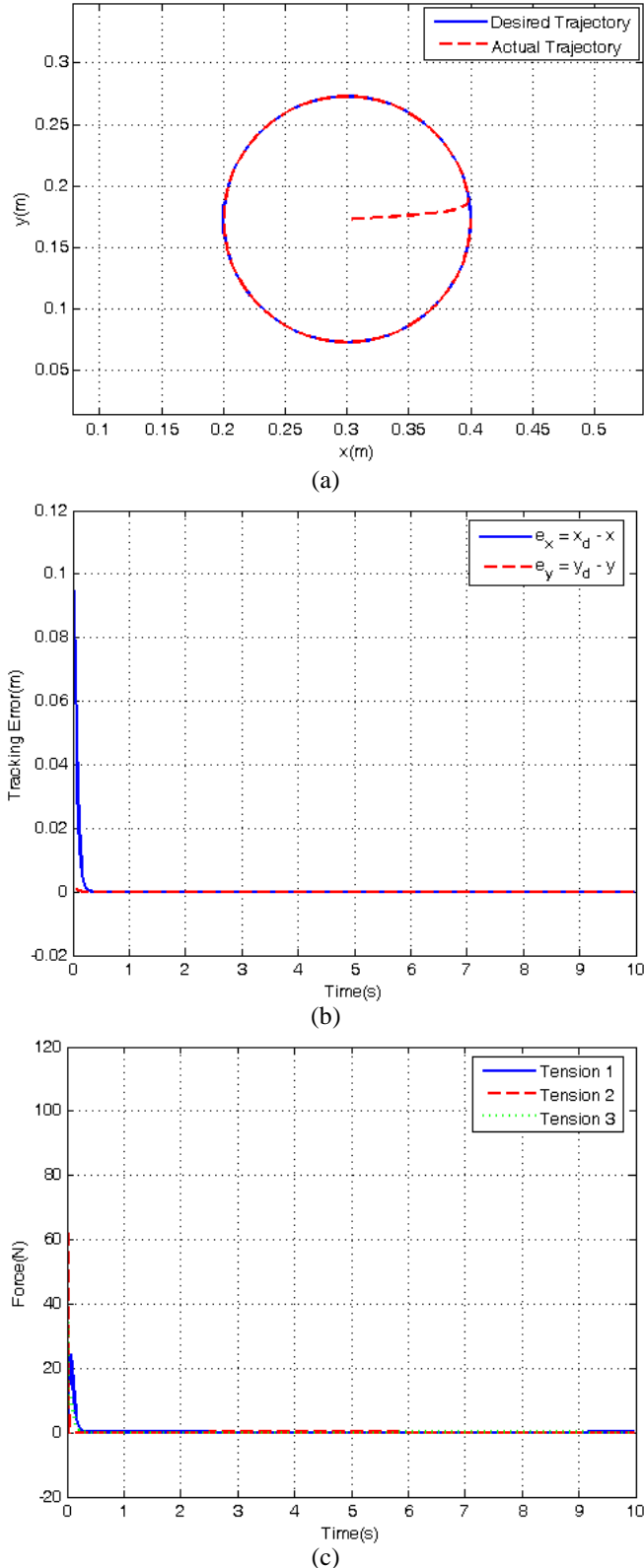


Fig. 5: (a) the circle trajectory use in the trajectory study; (b) the tracking error and (c) the tension force in the cable during the trajectory tracking.

## 5.2 Trajectory Tracking Study

In this simulation scenario, the end-effector is initially at  $(0.3, 0.173) m$  and the desired end-effector trajectory is a circle with trajectory  $x(t) = (0.3 + 0.1\cos(t)) m$ , and  $y(t) = (0.173 + 0.1\sin(t)) m$  (shown in Fig. 5(a)) such that the desired velocity is  $0.1 m/s$ . In Fig. 5(b) and (c), we can see the initial position converges to the desired trajectory asymptotically in very short time span. Moreover, the tension profile among cables that driving the end-effector shown in Fig. 5(c) are always positive, and they are being controlled to reduce to zero while the end-effector is converging to desired trajectory.

## 5.3 Trajectory Tracking with Stiffness Control

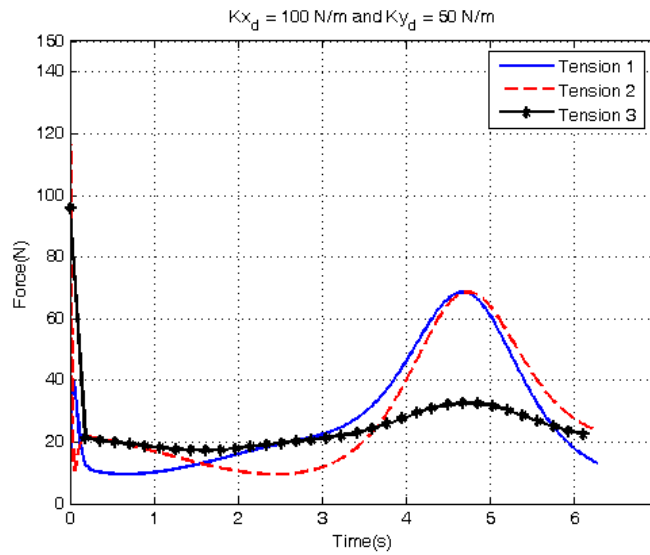
In this section, the simulation results show the performance of the point-mass cable robot implemented by trajectory tracking controller developed in Section 2 and the two active stiffness control schemes in Section 3. Without loss of generality, the stiffness constant of cables in all cases is set to  $1 N/m$ . The active stiffness schemes are briefly summarize as follows:

### 5.3.1 Weighted Stiffness Matrix:

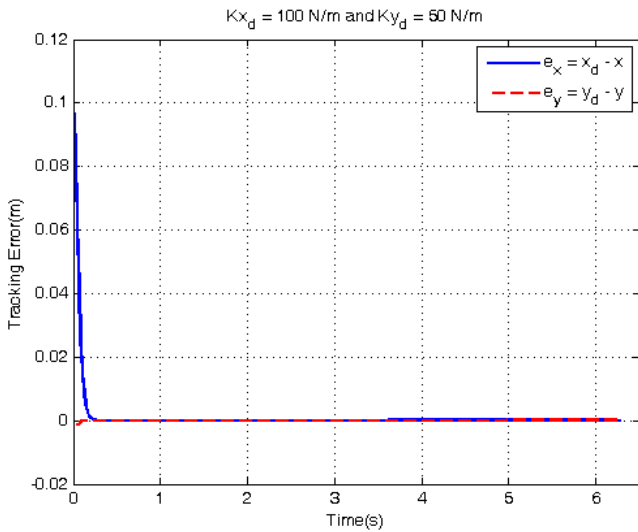
As mentioned earlier in Section 3.2, it is not always possible and necessary to realize the desired stiffness in all directions of end-effector (Cartesian space) of a cable robot system. Thus, we can achieve the control of stiffness in desired directions by assigning a weighting matrix to prioritize the elements in the stiffness matrix to be controlled. Specifically, in our work, we will only consider the diagonal elements in the stiffness matrix when formulating the weighting matrix, since the non-diagonal elements are highly coupled, and they have much less effect than the diagonal element to the overall stiffness of the workspace of cable robot system. The same circular trajectory (shown in Fig. 5(a)) is used for tracking.

### 5.3.2 Control of stiffness in X direction

In this case, the desired stiffness  $K_d = \text{diag}[K_{dx} K_{dy}] = [100 \ 50] N/m$ , we assume that the stiffness in  $x$  directions ( $K_x$ ) are primarily important. Hence, our goal is to reduce  $dK_x = (K_{dx} - K_x)$  with first priority. Accordingly, we set the weighting matrix in Eq.(33) as  $W = \text{diag}[1 \ 0 \ 0]$ , which means  $W_{k_x} = 1, W_{k_y} = 0$ . In Fig. 6 (b), we can see the end-effector tracks the desired trajectory very well, while the corresponding tension profile among cables that driving the end-effector shown in Fig. 6(a) are always positive. Moreover, in Fig. 7(a) and (b), we can see the stiffness in  $x$ -directions are at the desired stiffness  $100 N/m$  while the value of stiffness in  $y$ -directions is changing in a wide range, which is around from  $30 N/m$  to  $420 N/m$ .



(a)

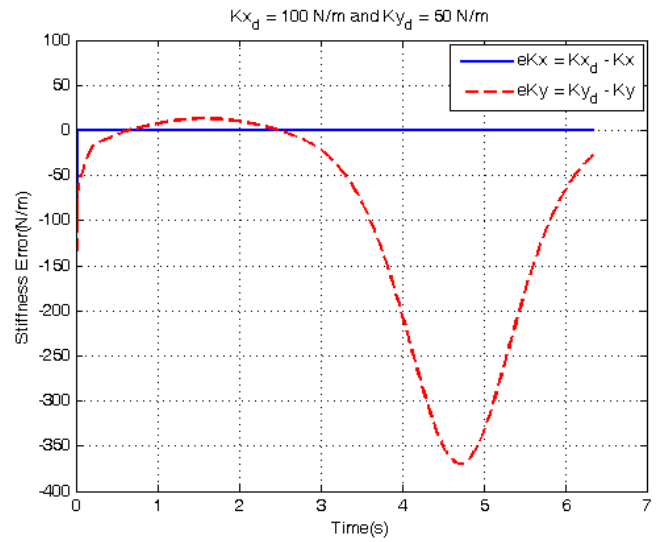


(b)

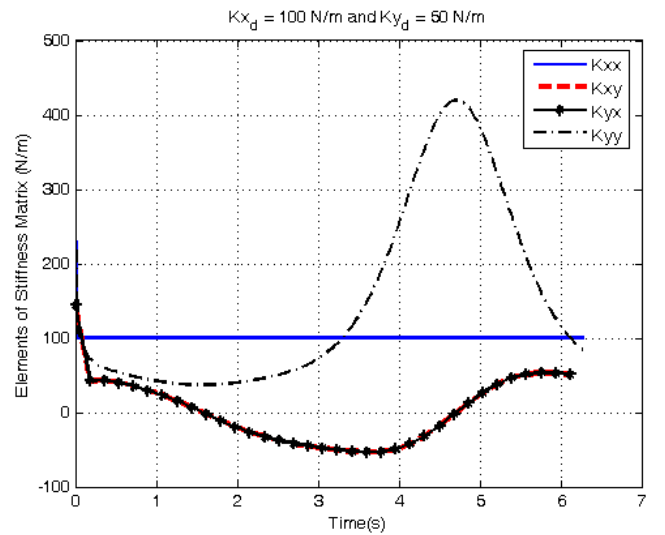
Fig. 6: (a) Tension force in the cables; and (b) Tracking errors.

### 5.3.3 Control of stiffness in both X and Y direction

In this case, the desired stiffness  $K_d = \text{diag}[K_{dx} \ K_{dy}] = [100 \ 50] \text{ N/m}$ , we assume that stiffness in both  $X$  and  $Y$  directions ( $K_x$  and  $K_y$ ) are equally important. Hence, our goal is to reduce  $dK_x = (K_{dx} - K_x)$  and  $dK_y = (K_{dy} - K_y)$  with equal priority. Accordingly, we set the weighting matrix in Eq.(33) as  $w = \text{diag}[\sqrt{0.5} \ 0 \ \sqrt{0.5}]$ , which means  $w_{K_x} = \sqrt{0.5}$ ,  $w_{K_y} = \sqrt{0.5}$ . In Fig. 8(b), we can see the end-effector tracks the desired trajectory very well, while the corresponding tension profile among cables that driving the end-effector shown in Fig. 8(a) are always positive. Moreover, in Fig. 9(a) and (b), we can see the stiffness in  $x$ -direction are near the desired stiffness 100 N/m. Meanwhile, the stiffness in  $y$ -direction is also near the desired stiffness 50 N/m, moreover, its error to the desired stiffness is less than that of in  $x$ -direction.



(a)



(b)

Fig. 7: (a) Stiffness error; and (b) Value of the stiffness matrix, in the control of stiffness in X direction case study.

## 6 DISCUSSION

The results shown in the two case studies (in Section 5.3) verify that the control schemes developed earlier are capable of achieving combinations of our goals: (i) trajectory tracking; (ii) achieving active (task space) stiffness control and (iii) optimizing cable force distribution. Trajectory tracking nonlinear controller based on feedback linearization technique provides good system performance to cable robots. Actuation redundancy provides feasible solution to address the control input constraint issue (in our case, positive tension force exerting by cables) in the control of cable robot system. Moreover, it provides flexibility and usability in the context of optimal cable force distribution and task space stiffness specification and adjustment.

Specifically, redundant actuation forces will not generate effective work in task space, but can generate and change task space stiffness of the system. The CCT based task space

stiffness mapping method [16] provides insight and understanding of relationship between redundant actuation forces and task space stiffness. Simulation results verify this assumption – larger task space stiffness can be achieved by higher level of redundant actuation forces in magnitude.

Disturbance-rejection issue in steady state can be effectively handled by means of active task space stiffness control, through the effect of restoring force term on position error.

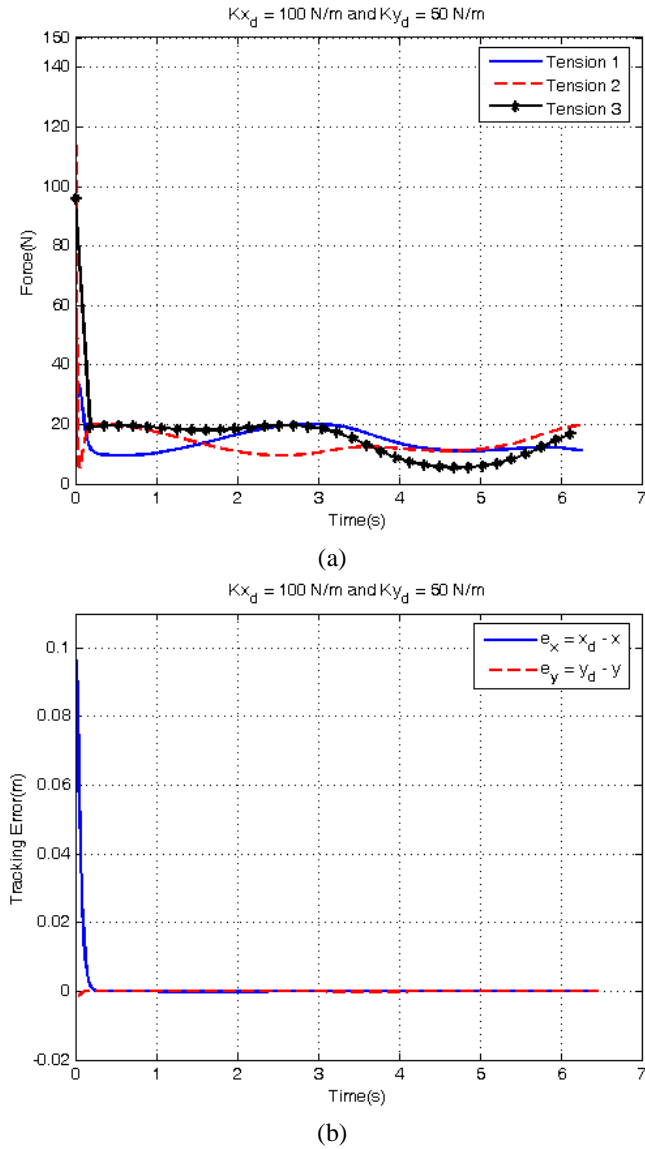


Fig. 8: (a) Tension force in the cables; and (b) Tracking errors.

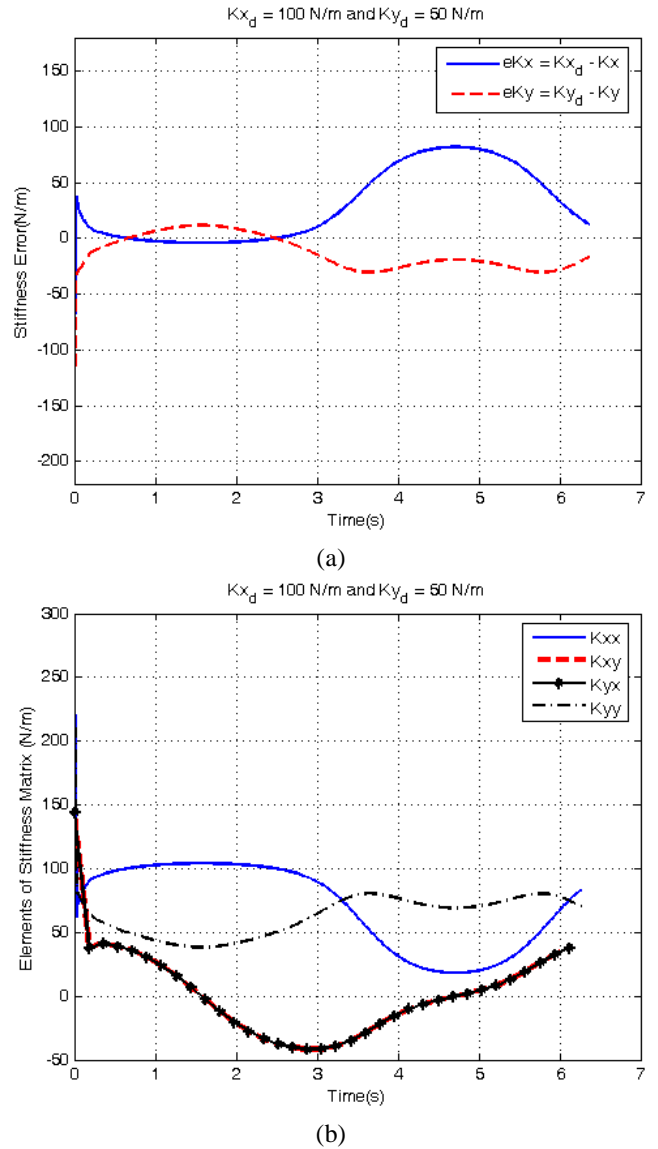


Fig. 9: (a) Stiffness error; and (b) Value of the stiffness matrix, in the control of stiffness in both X and Y direction case study.

## REFERENCES

- [1] Chakarov, D., 2004, "Study of The Antagonistic Stiffness of Parallel Manipulators with Actuation Redundancy," *Mechanism and Machine Theory*, 39(6), pp. 583-601.
- [2] O'Brien, J. F. and Wen, J. T., 1999, "Redundant Actuation for Improving Kinematic Manipulability," *Proc. IEEE International Conference on Robotics and Automation*, Detroit, Michigan, USA.
- [3] Nahon, M. A. and Angeles, J., 1989, "Force optimization in redundantly-actuated closed kinematic chains," *Proc. IEEE International Conference on Robotics and Automation*, Scottsdale, AZ, USA.
- [4] Yi, B. J., Freeman, R. A., and Tesar, D., 1989, "Open-loop stiffness control of overconstrained mechanisms/robotic linkage systems," *Proc. IEEE International Conference on Robotics and Automation*, Scottsdale, AZ, USA.

- [5] Ebert-Uphoff, I. and Voglewede, P. A., "On The Connections Between Cable-Driven Robots, Parallel Manipulators and Grasping," in *International Conference on Robotics & Automation*. New Orleans, LA, 2004.
- [6] Alp, A. B. and Agrawal, S. K., 2002, "Cable Suspended Robots: Feedback Controllers with Positive Inputs," *Proc. 2002 American Control Conference*, Anchorage, AK.
- [7] Behzadipour, S. and Khajepour, A., 2006, "Stiffness of Cable-based Parallel Manipulators with Application to the Stability Analysis," *ASME Journal of Mechanical Design*, 128(1), pp. 303-310.
- [8] Dagalakis, N. G., Albus, J. S., Wang, B. L., Unger, J., and D.Lee, J., 1989, "Stiffness Study of a Parallel Link Robot Crane for Shipbuilding Applications," *ASME Journal of Offshore Mechanics and Arctic Engineering*, 111(3), pp. 183-193.
- [9] Verhoeven, R., Hiller, M., and Tadokoro, S., 1998, "Workspace, stiffness, singularities and classification of tendon-driven stewart platforms," *Proc. 6th International Symposium on Advances in Robot Kinematics*, Salzburg, Austria.
- [10] Spong, M. W. and Vidyasagar, M., 1989, *Robot Dynamics and Control*. John Wiley and Sons,
- [11] Alp, A. B. and Agrawal, S. K., 2002, "Cable Suspended Robots: Design, Planning and Control," *Proc. IEEE International Conference on Robotics and Automation*, Washington, D.C.
- [12] Bullo, F. and Lewis, A. D., 2004, *Geometric Control of Mechanical Systems: Modeling, Analysis, and Design for Simple Mechanical Control Systems*. Springer,
- [13] Kumar, V. and Waldron, K. J., 1988, "Force Distribution In Closed Kinematic Chains," *Proc. IEEE International Conference on Robotics and Automation*.
- [14] Muller, A., 2005, "Internal Preload Control of Redundantly Actuated Parallel Manipulators & Its Application to Backlash Avoiding Control," *IEEE Transactions on Robotics and Automation*, 21(4), pp. 668-677.
- [15] Xiaoping, Y. and Sarkar, N., 1998, "Unified Formulation of Robotic Systems With Holonomic and Nonholonomic Constraints," *IEEE Transactions on Robotics and Automation*, 14(4), pp. 640-650.
- [16] Yanmei, L., Shih-Feng, C., and Imin, K., 2002, "Stiffness control and transformation for robotic systems with coordinate and non-coordinate bases," *Proc. IEEE International Conference on Robotics and Automation*, Washington D.C.
- [17] Salisbury, J. K., 1980, "Active Stiffness Control of A Manipulator in Cartesian Coordinates," *Proc. 19th IEEE Conference on Decision and Control including the Symposium on Adaptive Processes*, Albuquerque, NM.
- [18] Bhatt, R., Tang, C. P., Lee, L.-F., and Krovi, V., 2009, "A Case for Scaffolded Virtual Prototyping Tutorial Case-Studies in Engineering Education " *International Journal of Engineering Education*, 25(1), pp. 84-92.